Sensors and Materials, Vol. 38, No. # (2026) 1–13
MYU Tokyo

S & M ####

Design and Development of a Fuzzy-logic-based Long-range Aquaculture System

Sheng-Tao Chen[1*] and Tai-I Chou[2]

[1]Department of Avionics Engineering, Republic of China Air Force Academy, No. Sisou 1, Jieshou W. Rd., Kaohsiung City 820, Taiwan
[2]National Chung-Shan Institute of Science & Technology, Electronic Systems Research Institute, Quality Assurance Group, No. 481, Jia'an Section, Zhongzheng Rd., Taoyuan City 325, Taiwan

(Received October 21, 2024; accepted October 20, 2025)

Keywords: aquaculture system, LoRa, fuzzy controller, WSN, IoT

Water quality is essential for the survival of aquaculture species, making it a prominent issue in the aquaculture sector. Traditional aquaculture operations require substantial manpower and time to monitor water quality variations in fishponds, leading to operational challenges. An automated water quality monitoring system can relieve farmers of this burden and provide them with accurate information and assistance. Given the expansive nature of fishponds, it is necessary to employ long-range communication technologies to boost wireless signal coverage. Therefore, in this study, we incorporate a range of water quality sensors and LoRa long-range wireless communication technology to create a Fuzzy-logic-based Long-range Aquaculture System to address these issues. Upon deployment in fishponds, the system successfully monitored water quality and controlled dissolved oxygen levels. It is expected that this system will serve as a prototype for future aquaculture system innovations.

1. Introduction

Taiwan's traditional fishpond aquaculture relies heavily on farmers' experience to manage water quality and environmental conditions by monitoring parameters such as water temperature,[1–4] pH,[5–7] water level,[8] dissolved oxygen,[9,10] and salinity.[11] Aquaculture species are highly sensitive to even slight variations in these parameters, which can directly affect production efficiency and yield. However, traditional aerator controls, often based on experience, can result in aerators operating even after dissolved oxygen levels have reached saturation, leading to unnecessary energy consumption and increased farming expenses. Traditional aquaculture methods require constant monitoring and long hours of operation, which can place a considerable burden on farmers. As a result, the implementation of automation technology for accurate water quality monitoring to optimize the farming environment and reduce electricity consumption and labor costs has emerged as a major challenge in modern aquaculture.

*Corresponding author: e-mail: iiccanffly@gmail.com
https://doi.org/10.18494/SAM5406

ISSN 0914-4935 © MYU K.K.
https://myukk.org/

In the field of aquaculture automation, Singh *et al.* proposed an IoT-based intelligent monitoring and control system for freshwater recirculating aquaculture systems.[12] The system integrates multiple sensors and data analysis algorithms to control actuators for water quality regulation, with the goal of real-time monitoring and maintaining optimal water conditions.[12] Fu *et al.* proposed an intelligent water quality monitoring system for marine aquaculture based on a ZigBee backbone, where ZigBee is used to transmit water parameters to issue risk alerts.[1] Zou *et al.* integrated ZigBee with a 32-bit embedded controller to implement a fuzzy intelligent control system for aquaculture.[3] This system monitors water quality parameters to intelligently regulate the flow of micro-water and adopts an energy-saving wake-up strategy to manage sensor power supply.[3] Sung *et al.* utilized Wi-Fi to construct a wireless sensor network (WSN) and implemented real-time monitoring applications for aquaculture.[13] The literature highlights that, although some automated aquaculture technologies boost farming efficiency, most still encounter issues related to transmission distance and reliability, failing to adequately solve energy consumption and labor problems inherent in traditional aquaculture methods.[13]

The automated water quality monitoring and aerator control systems can effectively address the issues of energy waste and high labor demands associated with traditional aquaculture practices. These systems should feature real-time monitoring and intelligent decision-making capabilities to ensure that the farming environment remains optimal at all times. A critical component of the automated system is its ability to continuously monitor key water quality parameters such as dissolved oxygen, water temperature, pH, and salinity. From this data, the system can automatically adjust the relevant equipment, reducing the need for manual intervention and minimizing decision-making errors. Furthermore, the automated system should incorporate long-range, low-power data transmission technologies to enable broader application scenarios while reducing operational costs and energy consumption. By integrating fuzzy logic into the water quality decision-making process, traditional binary logic can be replaced with membership function values ranging from 0 to 1, providing a more nuanced description of water quality conditions.[14] Fuzzy logic is particularly well suited for representing the current status of water quality in fishponds, enabling the system to implement appropriate corrective actions as needed.

On the basis of the background of the aforementioned research, in this paper, we propose a Fuzzy-logic-based long-range Aquaculture System (FLAS) utilizing IoT technology. The goal is to overcome the transmission distance limitations of existing technologies while improving system reliability and energy efficiency. FLAS employs a LoRa communication module for the low-power, long-range data transmission of water quality measurements. The system's fuzzy logic controller determines the optimal timing for aerator activation based on real-time water quality data. This approach not only prevents energy waste from excessive aerator operation but also ensures that dissolved oxygen levels in the water are maintained, contributing to the modernization and sustainable development of the aquaculture industry.

2. Architecture

The architecture of FLAS is presented in Fig. 1. FLAS distinguishes between the fishpond sensing side, responsible for measuring water quality data, and the monitoring side at the backend, which collects and processes this information. The fuzzy controller subsequently generates outputs to manage the Aerator Control Side, ensuring optimal dissolved oxygen levels in the water.

2.1 Fishpond sensing side

FLAS integrates sensors for pH, dissolved oxygen, salinity, water temperature, water level, and environmental temperature/humidity to measure the water quality and environmental conditions of the fishpond. The collected data are transmitted to the monitoring side via LoRa wireless communication.

2.1.1 Sensors

The fishpond sensing side employs multiple high-precision sensors to measure six types of water quality data, including pH. These data are used to represent the overall water quality and environmental conditions of the fishpond. The sensors utilized in this study are listed in Table 1.

2.1.2 Microcontroller

In addition to utilizing six sensors to measure water quality and environmental conditions in the fishpond, the sensing side also employs a LoRa module for data transmission. Therefore, in this study, we adopted the Arduino Mega 2560 microcontroller,[21] which provides a higher number of I/O interfaces, to integrate these devices.

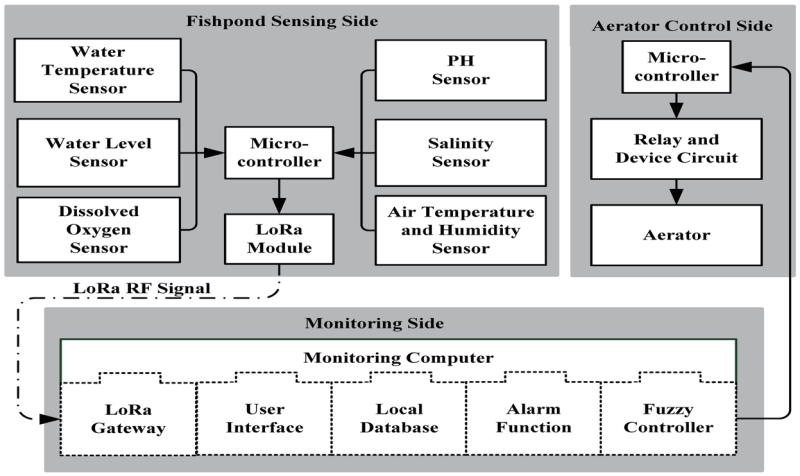

Fig. 1. Architecture diagram of FLAS (adapted from Ref. 25).

Table 1
Integrated sensors in FLAS.

Sensor	Model	Measurement information (range)	Accuracy
pH	SEN161[15]	pH (0 to 14)	±0.1
Dissolved oxygen	EZO-DO[16]	Dissolved oxygen (0 to 100 ppm)	±0.05 ppm
Salinity	Electrical conductivity[17]	Electrical conductivity (0 to 20 mS/cm)	±5% FS
Water temperature	DS18B20[18]	Water temperature (−55 to +125 °C)	±0.5 °C
Water level	9550[19]	Water level (0 to 3 m)	<0.1% FS
Environmental temperature/humidity	DHT22[20]	Air temperature (−40 to 80 °C) Air humidity (0 to 100% RH)	Temperature: ±0.5 °C Humidity: ±2–5% RH

2.1.3 LoRa wireless module

The LoRa wireless module used in this study is iL-LoRa 1272, which can achieve a transmission distance of more than 15 km in suburban areas.[22] FLAS utilizes iL-LoRa 1272, which operates in the low-frequency 915 MHz band and has a standby current of less than 1 μA, making it ideal for long-distance, low-power wireless communication applications.

2.2 Monitoring side

Visual Studio C# was used to develop the user interface (UI) for FLAS, while the aerator control in FLAS was implemented using Matlab R2017 to design the fuzzy controller.

2.2.1 Fuzzy controller

In the FLAS fuzzy controller, Matlab is used to perform fuzzy operations such as "fuzzification", "rule base establishment", "fuzzy inference", and "defuzzification" to generate the final output indicators. As shown in Fig. 2, the inputs to the fuzzy controller include the dissolved oxygen level at the water surface (DO), bottom water temperature (T0), pH, and salinity (S), while the output corresponds to the operational status of the aerator (Aerator). Here, the parentheses for the output and input indicate the variable names.

In this study, we utilized the triangular membership function (Trimf) to convert clear input values into fuzzy values between 0 and 1. Equation (1) represents this membership function $\mu(x)$.

$$\mu(x)=\begin{cases}0, & \text{if } x \le a \text{ or } x \ge c \\ \dfrac{x-a}{b-a}, & \text{if } a \le x \le b \\ \dfrac{c-x}{c-b}, & \text{if } b \le x \le c\end{cases} \tag{1}$$

Here, a, b, and c represent the three vertices of the triangular membership function, which are used to design the fuzzy membership relationship. On the other hand, the coefficients for the relevant inputs and outputs are defined in Table 2.

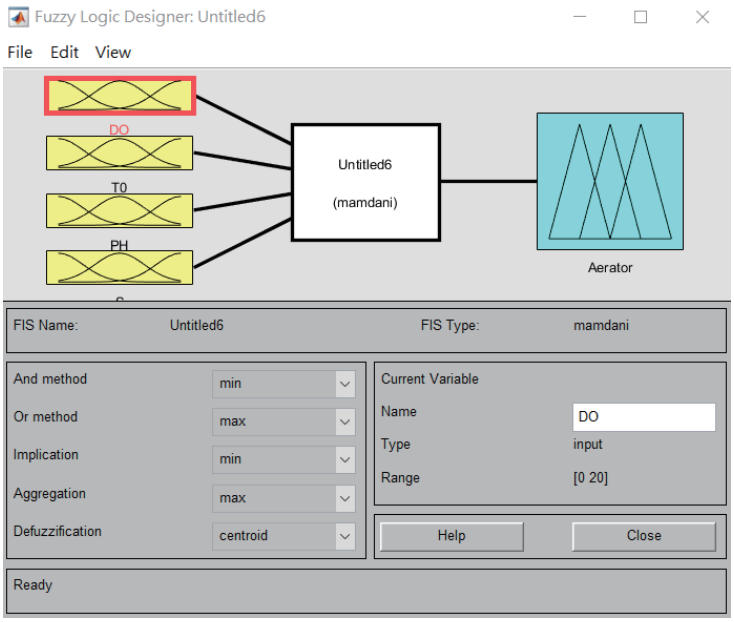

Fig. 2. (Color online) Design of the fuzzy controller.

Table 2
Input and output definitions.

Variable	No.	Name (unit)	Value range definition			
Input	1	*DO* (ppm)	State	Very low	Low	Normal
			Range	$DO \leq 3$	$3 < DO \leq 6$	$5 < DO \leq 20$
	2	*T*0 (°C)	State	Low	Normal	High
			Range	$T0 \leq 20$	$20 < T0 \leq 32$	$32 < T0 \leq 50$
	3	*PH* (-)	State	Low	Normal	High
			Range	$PH \leq 7$	$6 < PH \leq 9$	$8 < PH \leq 14$
	4	*S* (mS/cm)	State	Low	Normal	High
			Range	$S \leq 0.7$	$0.7 < S \leq 1.5$	$1.45 < S \leq 2$
Output	1	*Aerator*	State	OFF	ON	–
			Range	$Aerator \leq 0.32$	$0.3 < Aerator \leq 1$	–

After consultations with experienced aquaculture experts in Chiayi County, Taiwan, each with over 20 years of farming experience in white shrimp and milkfish, we developed a rule base of 81 fuzzy rules. The experts' practical knowledge guided the definition of input–output relationships under varying conditions of dissolved oxygen, temperature, pH, and salinity. The rule base was then configured and refined through MATLAB simulations of multiple water quality scenarios to ensure that the inferred aerator operations aligned with the experts' recommendations. This design enables the fuzzy controller to infer the activation strength using the minimum value for the AND operation, as shown in Eq. (2).

$$\mu_{activation} = \min\left(\mu_{A_1}(x_1), \mu_{A_2}(x_2), \mu_{A_3}(x_3), \cdots \mu_{A_n}(x_n)\right) \tag{2}$$

Here, A_1, A_2, …, A_n represent the fuzzy sets of input variables, and $\mu_{activation}$ denotes the activation strength of the rules. Furthermore, the "max-min composition method" of the Mamdani fuzzy model is employed for fuzzy inference. Finally, Eq. (3) represents the Center of Gravity (CoG) method used in this study for defuzzification, resulting in a clear quantifiable output that serves as the control command for the aerator.

$$y = \frac{\int_{y_{min}}^{y_{max}} y \cdot u_B(y)\,dy}{\int_{y_{min}}^{y_{max}} u_B(y)\,dy} \tag{3}$$

Here, y is the clear output for controlling the aerator, B is the fuzzy set of the output variable, and $u_B(y)$ is the corresponding fuzzy membership function for the output variable. y_{max} and y_{min} denote the upper and lower bounds of the output range. Subsequently, using the input data [*DO*, *T*0, *PH*, *S*] = [10, 25, 7, 1] as an example, the fuzzy controller processes the information and yields the results shown in Fig. 3, indicating that the aerator output is 0.16, signifying an off state.

2.2.2 User interface and LoRa gateway

The monitoring computer integrates the iL-LoRa 1272 gateway to receive water quality information from the fishpond sensing side, enabling users to monitor the current water quality data in real time, as shown in Fig. 4(a). Additionally, Fig. 4(b) shows the UI of FLAS, which provides the real-time visualization of the water quality information.

2.2.3 Alarm function and database

Dissolved oxygen is the most critical parameter affecting water quality. Insufficient dissolved oxygen levels can cause immediate harm to aquatic life in fishponds. Figure 5 illustrates the

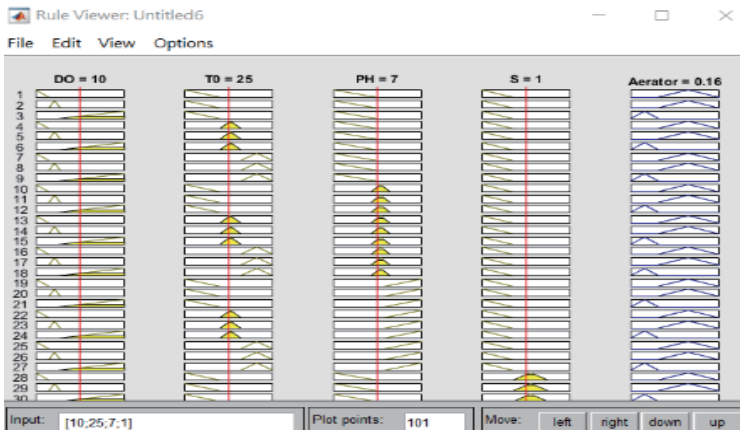

Fig. 3. (Color online) Fuzzy logic inference results.

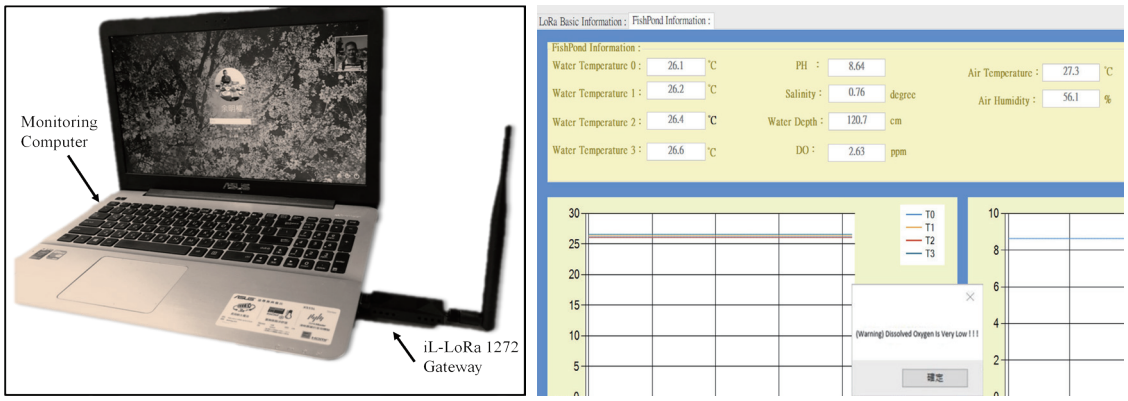

(a) (b)

Fig. 4. (Color online) (a) Monitoring computer and LoRa gateway. (b) User interface of FLAS.

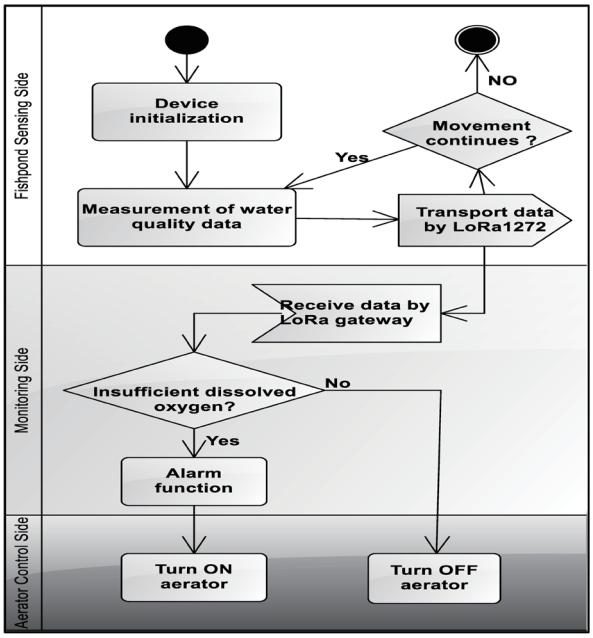

Fig. 5. Alarm function flowchart.

alarm function workflow, which is activated when the dissolved oxygen levels in the fishpond are inadequate. In addition to using Microsoft Access to implement a local database for recording data, FLAS also employs Google Spreadsheet to create a cloud database.

2.3 Aerator control side

The aerator control side and the monitoring computer are both located within the power control room. The electrical wiring for the fishpond controls multiple aerators, each consuming 746 W per hour. The monitoring computer activates the corresponding aerator by switching the state of the solid-state relay via the MCU, which in turn controls the distribution panel circuit. Figure 6 illustrates the setup of the aerator control side.

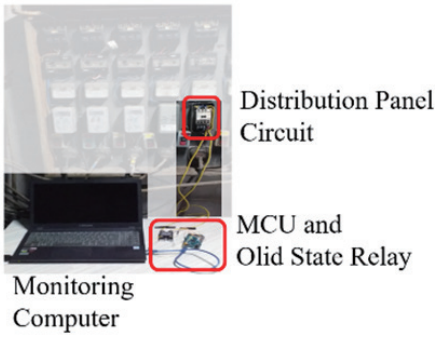

Fig. 6. (Color online) Monitoring computer and aerator control side.

3. Experiments

In this section, we will describe how FLAS was installed in the fishpond to conduct experiments, serving as the foundation for subsequent analysis and discussion.

3.1 Experimental setup

The field experiment was conducted at commercial fishponds in Chiayi City, Taiwan, where white shrimp and milkfish are routinely cultured. Following our prior study,[25] the fishpond sensing device (equipped with pH, dissolved oxygen, salinity, water temperature, water level, and air temperature/humidity sensors) was deployed on the pond levee, while the monitoring computer and LoRa gateway were installed in the power-control room. As illustrated in Fig. 7, the sensing device was mounted in a weatherproof enclosure with probes immersed at manufacturer-recommended depths. The relative distance between the sensing device and the monitoring side was approximately 200 m (Fig. 8).

3.2 Experimental scenarios

In Cases 1, 2, and 3, the experimental scenarios comprised 300000 shrimp, 600000 shrimp, and 600000 shrimp combined with 5500 milkfish, respectively. These scenarios were determined in consultation with aquaculture practitioners to capture representative biomass levels and mixed-species farming conditions. In each case, dissolved oxygen was sampled at 1 min intervals for 120 min under two operational phases: aerator-on and aerator-off. Owing to operational constraints at the commercial pond (e.g., continuous production and limited intervention windows), each case was recorded once (single field run per phase).

To avoid overstating the degrees of freedom, minute-wise observations were not treated as independent replicates. Instead, each trajectory was summarized using curve-level metrics, and uncertainty was estimated via a residual-preserving block bootstrap (10 min blocks; 1000 resamples) to derive 95% confidence intervals and one-way analysis of variance (ANOVA) with Tukey post-hoc comparisons, which respects temporal autocorrelation. Specifically, for the

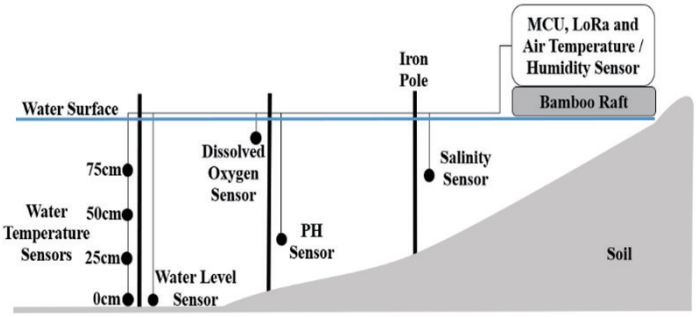

Fig. 7. (Color online) Monitoring device configuration diagram (adapted from Ref. 25).

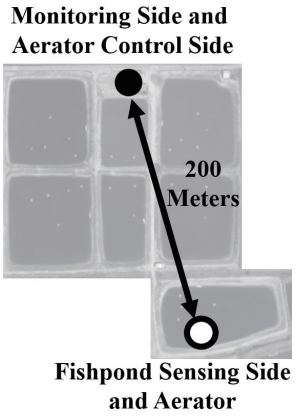

Fig. 8. Relative position diagram of the fishpond.

aerator-on phase, we report the initial 0–20 min slope and the time-to-threshold metrics T_6 (6 ppm) and T_7 (7 ppm); for the aerator-off phase, we report the 0–60 min decline slope and the 120-min-depletion area-under-the-curve (AUC). Group comparisons across cases were then performed on the bootstrap replicates.

4. Results and Discussion

Figure 9 presents the minute-by-minute decline in dissolved oxygen over 120 min. Case 3 exhibits the most rapid depletion and approaches 3 ppm earlier than the other groups, whereas Case 1 declines most slowly and Case 2 lies between them. To avoid pseudoreplication, we summarize each trajectory using curve-level metrics. The decline slopes over 0 to 60 min were −0.032, −0.033, and −0.037 ppm/min in Cases 1, 2, and 3, respectively; the 120-min-depletion AUCs were 209.4, 232.8, and 249.8 ppm·min in the same order. ANOVA based on bootstrap replicates indicated no significant between-case effect for either metric (slope: $F = 2.45$, $p = 0.087$; AUC: $F = 0.18$, $p = 0.832$).

Dissolved oxygen recovery after aeration is shown in Fig. 10. The initial increases during the first 20 min were 0.102, 0.098, and 0.040 ppm/min in Cases 1, 2, and 3, respectively, indicating

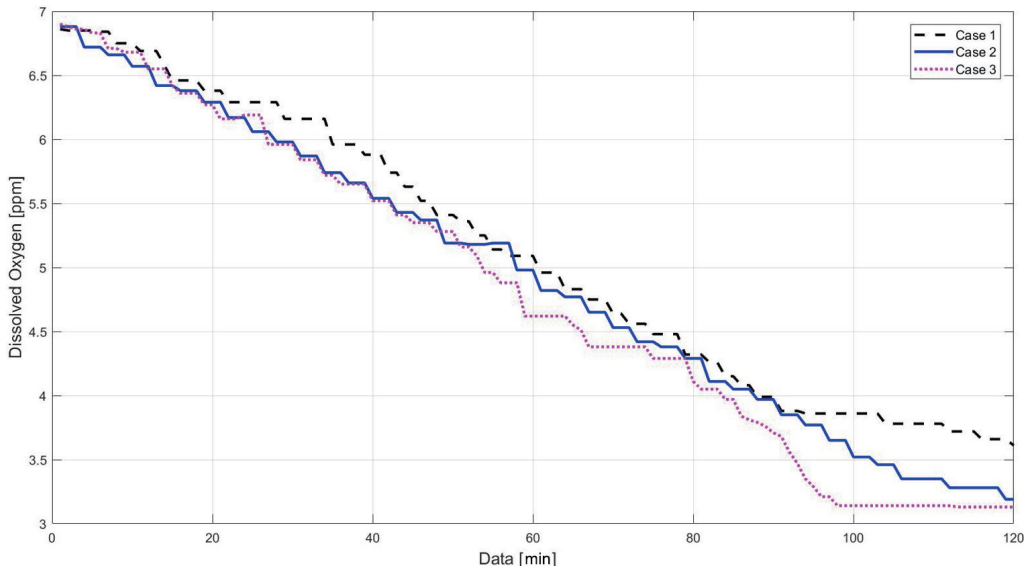

Fig. 9. (Color online) Decline in dissolved oxygen level.

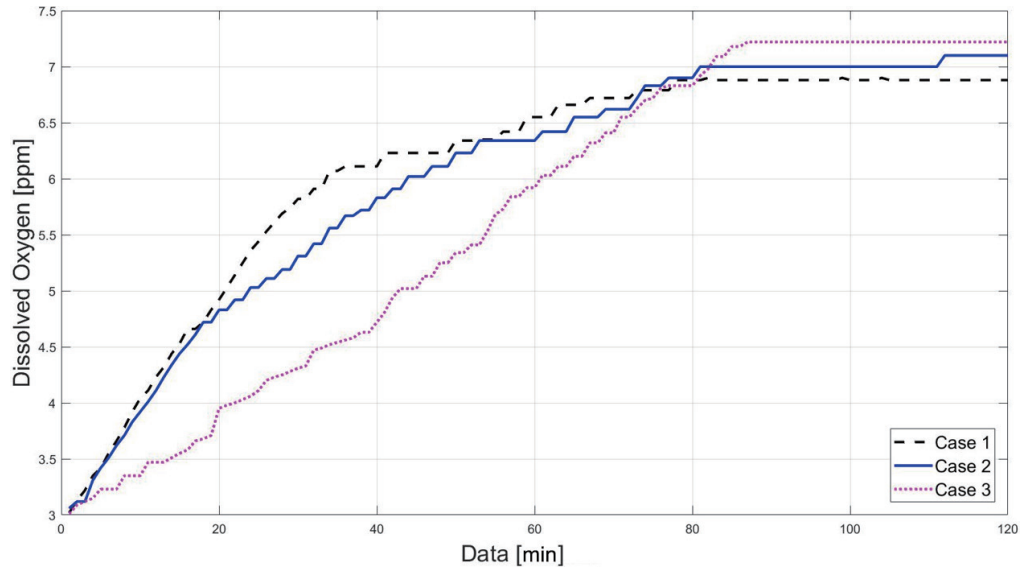

Fig. 10. (Color online) Increase in dissolved oxygen level with aerator activated.

comparable early-phase rates in Cases 1 and 2 and a lower early-phase rate in Case 3. The times to 6 ppm (T_6) were 33, 43, and 60 min, with a significant between-case effect (ANOVA F = 87.97, $p < 1 \times 10^{-36}$; Tukey's HSD: all pairwise $p < 0.001$). For the time to 7 ppm (T_7), Cases 2 and 3 reached 7 ppm at 80 and 82 min, respectively, whereas Case 1 did not reach 7 ppm within 120 min (right-censored and reported as ">120 min"); the between-case difference in T_7 was not significant.

From the experimental and statistical results, the DO trajectories show that stocking composition and density primarily determine the speed of recovery to an operationally safe

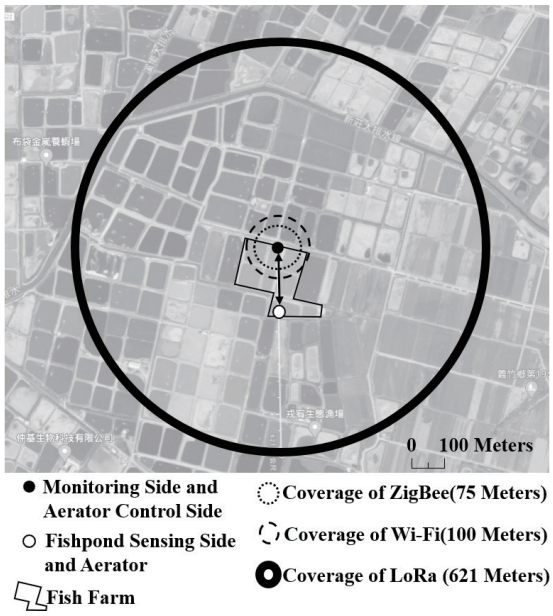

Fig. 11. Transmission range and comparative coverage.

level, with T_6 (time to 6 ppm) providing the most discriminative and operationally relevant indicator under this field setting, whereas decline-phase metrics do not differ significantly across cases. Beyond these primary findings, the minute-wise series also reveals qualitative co-variation consistent with aquaculture physiology and our fuzzy design: higher water temperature and salinity are associated with tighter DO safety margins, and departures of measured pH from the neutral range tend to coincide with slower DO recovery. These relations are implicitly encoded in the membership partitions and antecedent structure of the DO–T_0–PH–S rule base. Given the single-run limitation, we refrain from formal multi-factor correlation/effect decomposition; replicated multi-pond, multi-season campaigns will enable rigorous correlation modeling in future work.

Moreover, the LoRa module achieved an effective transmission distance of 621 m, as referenced from previous experimental results.[23] Figure 11 illustrates the actual experimental scenario, showing that FLAS significantly outperforms Wi-Fi with a range of 100 m and ZigBee with a range of 75 m.[24] In addition, LoRa exhibits lower power consumption per transmission (less than 50 mW) than Wi-Fi (more than 200 mW) and ZigBee (about 100 mW). This advantage directly reduces the overall system energy demand, which is critical for long-term aquaculture deployment. Consequently, FLAS offers clear advantages for water-quality monitoring in large fishponds that require reliable long-range, low-power data links.

5. Conclusions

In this study, we presented FLAS, an automated aquaculture water-quality system that integrates multi-parameter sensing with long-range LoRa communication and fuzzy-logic

control. Deployed in a commercial fishpond in Chiayi, Taiwan, the system reliably captured dissolved oxygen dynamics under aerator-off depletion and aerator-on recovery, and actively improved water quality via data-driven aerator actuation. Curve-level analyses established that stocking composition and density primarily affect recovery speed to operational safety, underscoring the value of responsive control in real-world ponds. Beyond the field trial, FLAS offers practical pathways for scaling: multi-pond networking over long distances, energy-aware aeration to reduce operating costs, predictive control using historical time series, and integration with cloud/edge dashboards for real-time decision support and alerts. Future work will extend evaluation with replicated trials across seasons and species mixes, broaden the rule base with expert-informed or data-driven optimization, and incorporate additional sensors (e.g., ammonia and nitrite) to support comprehensive health management and sustainability reporting. Taken together, these advances position FLAS as a deployable foundation for intelligent, resilient, and cost-effective aquaculture operations.

Acknowledgments

The authors would like to thank the anonymous reviewers of their paper for the many helpful suggestions. This work was partially supported by the National Science and Technology Council (NSTC), Taiwan, under grant number 113-2222-E-013-001. The authors would like to acknowledge the original development team of the preliminary water quality monitoring infrastructure, the early stages of which were presented at ISPACS 2021.[25]

References

1 Y. Fu, Y. Liu, D. Wang, K. Liu, X. Li, J. Xu, and Z. Wu: Proc. 2023 IEEE 11th Joint Int. Inf. Technol. and Artif. Intell. Conf. (ITAIC, Chongqing, China, 2023) 1695–1699. https://doi.org/10.1109/ITAIC58329.2023.10408905
2 C. Encinas, E. Ruiz, J. Cortez, and A. Espinoza: Proc. 2017 Wireless Telecommun. Symp. (WTS, Chicago, IL, USA, 2017) 1–7. https://doi.org/10.1109/WTS.2017.7943540
3 Z. Zou, R. Liu, Y. Wang, P. Huang, and L. Xu: Proc. 2023 IEEE 7th Inf. Technol. and Mechatron. Eng. Conf. (ITOEC, Chongqing, China, 2023) 464–468. https://doi.org/10.1109/ITOEC57671.2023.10291527
4 B. Shi, V. Sreeram, D. Zhao, S. Duan, and J. Jiang: Biosyst. Eng. **172** (2018) 57. https://doi.org/10.1016/j.biosystemseng.2018.05.016
5 F. A. B. G. Pratama, F. Hidayatullah, E. L. I. P. Sari, I. K. A. Enriko, F. N. Gustiyana, and A. Luthfi: Proc. 2024 Int. Conf. Green Energy, Comput. and Sustainable Technol. (GECOST, Miri, Sarawak, Malaysia, 2024) 72–76. https://doi.org/10.1109/GECOST60902.2024.10474710
6 G. Wiranto, Y. Y. Maulana, I. D. P. Hermida, I. Syamsu, and D. Mahmudin: Proc. 2015 Int. Conf. on Smart Sens. and Appl. (ICSSA, 2015) 111–115. https://doi.org/10.1109/ICSSA.2015.7322521
7 C. S. Liu, X. T. Chen, W. Y. Shih, C. C. Lin, J. H. Yen, C. J. Huang, and Y. T. Yen: Sens. Mater. **35** (2023) 3019. https://doi.org/10.18494/SAM4513
8 J. H. Chen, W. T. Sung, and G. Y. Lin: Proc. 2015 IEEE Int. Conf. on Syst., Man, and Cybern. (SMC, Kowloon, China, 2015) 1161–1166. https://doi.org/10.1109/SMC.2015.208
9 T. L. Ngoc, C. Vo, and P. Talbot: Proc. 2025 Int. Conf. on Emerging Technol. and Comput. (IC_ETC, Brest, France, 2025) 1–5. https://doi.org/10.1109/IC_ETC65981.2025.11141295
10 Y. Ma and W. Ding: Proc. 2018 IEEE 3rd Adv. Inf. Technol., Electron. and Autom. Control Conf. (IAEAC, Chongqing, China, 2018) 414–418. https://doi.org/10.1109/IAEAC.2018.8577649
11 R. Adriman, M. Fitria, A. Afdhal, and A. Y. Fernanda: Proc. 2022 IEEE Int. Conf. on Commun., Networks and Satell. (COMNETSAT, Solo, Indonesia, 2022) 356–360. https://doi.org/10.1109/COMNETSAT56033.2022.9994388
12 M. Singh, K. S. Sahoo, and A. H. Gandomi: IEEE Internet Things J. **11** (2024) 4206. https://doi.org/10.1109/JIOT.2023.3298844

13 W.-T. Sung, I. G. T. Isa, and S.-J. Hsiao: Sens. Mater. **36** (2024) 1019. https://doi.org/10.18494/SAM4660
14 L. Zadeh: Inf. Control **8** (1965) 338. https://doi.org/10.1016/S0019-9958(65)90241-X
15 Sonde pH + interface SEN0161: https://www.gotronic.fr/art-sonde-ph-interface-sen0161-21552.htm (accessed October 20, 2024).
16 Atlas Scientific: https://www.atlas-scientific.com/_files/_datasheets/_circuit/DO_EZO_Datasheet.pdf (accessed October 20, 2024).
17 Gravity: Analog Electrical Conductivity Sensor: https://www.dfrobot.com/product-1123.html?search=Analog%20Electrical%20Conductivity%20Sensor (accessed October 20, 2024).
18 DS18B20: https://datasheets.maximintegrated.com/en/ds/DS18B20.pdf (accessed October 20, 2024).
19 9550 Pressure Transducer: http://geostar.com.tw/index.php/pressure_transducer/9550_pressure_transducer (accessed October 20, 2024).
20 DHT22 Temperature-Humidity Sensor: https://www.inventelectronics.com/product/dht22-temperature-humidity-sensor/ (accessed October 20, 2024).
21 Arduino: https://store.arduino.cc/products/arduino-mega-2560-rev3?srsltid=AfmBOor9-4zxn3Wkelqlww1_Vy6f2vwGvhcmWPw11dYA55WncFPkH7rr (accessed October 20, 2024).
22 IFROGLAB: https://www.ifroglab.com/tw/?p=7086 (accessed October 20, 2024).
23 S. S. Lin, C. W. Lan, S. T. Chen, and K. C. Li: Sens. Mater. **32** (2020) 2057. https://doi.org/10.18494/SAM.2020.2786
24 Y. Song, J. Lin, M. Tang, and F. Dong: Eng. **3** (2017) 460. https://doi.org/10.1016/J.ENG.2017.04.011
25 S. T. Chen, S. S. Lin, C. W. Lan, and T. I. Chou: Proc. 2021 Int. Symp. on Intell. Signal Process. and Commun. Syst. (ISPACS 2021, Hualien, Taiwan, 2021) 1–2. https://doi.org/10.1109/ISPACS51563.2021.9651127

About the Authors

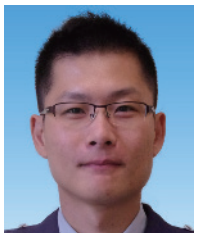

Sheng-Tao Chen is an assistant professor in the Republic of China Air Force Academy, Taiwan. He received his M.S. degree from the Department of Information Management, and the School of Defense Science, Management College, National Defense University Taipei, Taiwan, in 2013 and his Ph.D. degree from the Department of Electrical and Electronic Engineering of Chung Cheng Institute of Technology, National Defense University, Taoyuan, Taiwan, in 2020. His research interests include AIoT, wireless sensor networks, and computer vision. (iiccanffly@gmail.com)

Tai-I Chou received his B.S. degree from the Department of Electrical Engineering of the Chinese Culture University in 2017 and his M.S. degree from the National Defense University Institute of Technology in 2019. His research interests include digital control, wireless sensor network technology and application, automation control, and IOT application system development. (zu0035144440@gmail.com)